ELSEVIER

Journal of Organometallic Chemistry 497 (1995) 181–193

Journal of Organometallic Chemistry

Crystal structure and propene polymerization characteristics of bridged zirconocene catalysts ☆

W. Kaminsky [a,*], O. Rabe [a], A.-M. Schauwienold [a], G.U. Schupfner [a], J. Hanss [b], J. Kopf [b]

[a] *Institut für Technische und Makromolekulare Chemie, Bundesstraße 45, Universität Hamburg, D-20146 Hamburg, Germany*
[b] *Institut für Anorganische und Angewandte Chemie, Martin-Luther-King Platz 6, Universität Hamburg, D-20146 Hamburg, Germany*

Received 7 February 1995

Abstract

The synthesis, crystal structure and propene polymerization behaviour of four bridged zirconocene dichlorides is presented. All catalysts are capable of isotactic propene polymerization. Methyl substitutions at the 2-, 4- and 7-positions of the bridged bis(indenyl)zirconocene dichlorides were introduced. The methyl substituent in the 7-position of the indenyl ring induces a significant steric interaction with the bridging group. On comparison of the 2,4,7-methyl substituted catalysts with their unsubstituted counterparts, only the ethylidene bridged catalyst *rac*-1,2-ethylidene-bis(2,4,7-trimethyl-1-indenyl)zirconium dichloride (**4**) is forced into the optimum geometry for isotactic propene polymerization. Owing to the steric bulk at the bridge catalyst **4** is very rigid with respect to the movement of the indenyl rings and the metal centre thus produces highly isotacic polypropene even up to high polymerization temperatures. Molecular mechanics calculations and temperature-dependent NMR measurements demonstrate that catalyst **4** is not able to equilibrate between the λ and δ conformational state as the corresponding *rac*-1,2-ethylidene-bis(-1-indenyl)zirconium dichloride (**3**) catalyst does. In the case of the catalyst isopropyliden((3-*tert*-butyl)cyclopentadienyl-9-fluorenyl)zirconium dichloride (**6**) the substitution in the 3-position changes the symmetry from C_s to C_1. This catalyst produces isotactic polypropene but with a decreased polymerization activity.

Keywords: Zirconocene; Homogeneous Ziegler–Natta catalysis; Propene polymerization; Molecular mechanics calculations

1. Introduction

Following the discovery of isotactic propene polymerization by *ansa* zirconocenes [1], many attempts have been made to improve the properties of the resulting polymers such as melting point and molecular weight.

Substituted bridged bis(indenyl) catalysts are known to be prepared or cleaned by fractional crystallization to yield a great excess of the racemic metallocene isomer over the unwanted *meso* isomer [2]. Therefore indenyl catalysts have so far been a preferred target in the field of catalyst research in homogeneous Ziegler–Natta catalysis. As a straightforward way for tuning the catalyst performance it appeared to many that the whole ligand framework did not need to be changed but only the substitution patterns of the indenyl ring need to be modified.

Modifications on the bridge in general did not increase the selectivity or molecular weight significantly [3,4] while methyl substitution in the 2-position of the cyclopentadienyl ring resulted in a lower rate of chain transfer, thus leading to polypropene of a higher molecular weight [5]. However, so far in comparison with conventional polypropene made by heterogeneous Ziegler–Natta catalysts the polypropene lacked a comparably high melting point; even so the isotacticity measured in terms of mmmm pentad concentration is above that of the conventional polypropene [6]. This phenomenon could only be understood by the contribution of other regiodefects in the polymer such as 2,1 insertions and 1,3 insertions [7] that are much fewer in number but nevertheless cause more hindrance to chain folding and crystallization than do the more frequent racemic defects [8]. A comparison of regiodefects and

☆ Dedicated to Professor Hans-H. Brintzinger on the occasion of his 60th birthday.

* Corresponding author.

Elsevier Science S.A.
SSDI 0022-328X(95)00123-9

stereodefects in polypropene polymerization for five different *ansa*-bisindenyl catalysts at 0, 30 and 60 °C polymerization temperature has been published elsewhere [9].

A possible solution for a higher regioselectivity cannot only be a sterically optimized coordination site to force the incoming monomer into a coordination suitable for 1,2 insertion. For molecular weight control the growing polymer chain must be in the right orientation to favour isotactic enchainment over possibly β-hydride-mediated chain termination reactions of the polymer chain. Both aspects of geometry are strongly dependent on the steric demand of the oriented olefin and polymer chain in the fairly small coordination gap. Therefore a rising flexibility of the ligand framework induced by an enhanced polymerization temperature may destroy the preferred mode of catalyst geometry and leads to a drastic decrease in polymer selectivity with increasing polymerization temperature.

As a general consideration it was known that a 2-methyl substitution increases the molecular weight, while a 3-methyl substitution leads to an unsatisfactory low isotacticity of the polymer (see Table 2 later and the literature cited therein). The influence of a substitution on the 4- and 7-positions to the polymer were at that time not yet known. It was estimated that a 4-methyl group could have an influence on the regiocontrol, thus reducing the rate of 2,1-olefin insertions, and a 7-methyl group should increase the steric bulk on the bridge, resulting in an enhanced rigidity possibly accompanied by a twist of the indenyl ring systems.

The aim of this work was to synthesize a substituted indenyl-ligand featuring an optimized catalyst geometry and inducing sufficient rigidity to the movement of the indenyl rings to ensure stereoselectivity and regioselectivity even at high polymerization temperatures.

It was only recently that Spaleck et al. [10] and Brintzinger and coworkers [11] succeeded in synthesizing aromatic substituted or annealed indenyl zirconocenes, which are capable of producing polypropene with a high molecular weight, a high activity and high melting points (158–161 °C and 152 °C) at polymerization temperatures of 60 °C and 50 °C, respectively. In this work the first ethylene-bridged indenyl catalyst to produce polypropene with similar properties is presented.

Modification of the well-known [$Me_2C(Cp)(Fluo)$] $ZrCl_2$ system [12–14] by a *tert*-butyl group at the 3-position in the Cp ring leads to a metallocene with interesting stereochemistry. [Me_2C(*tert*-BuCp)(Fluo)] $ZrCl_2$ was first synthesized by Ewen and Elder [15] and reported to yield isotactic polypropene whereas the unsubstituted system produces a polymer with syndiotactic microstructure. That the frequently troublesome

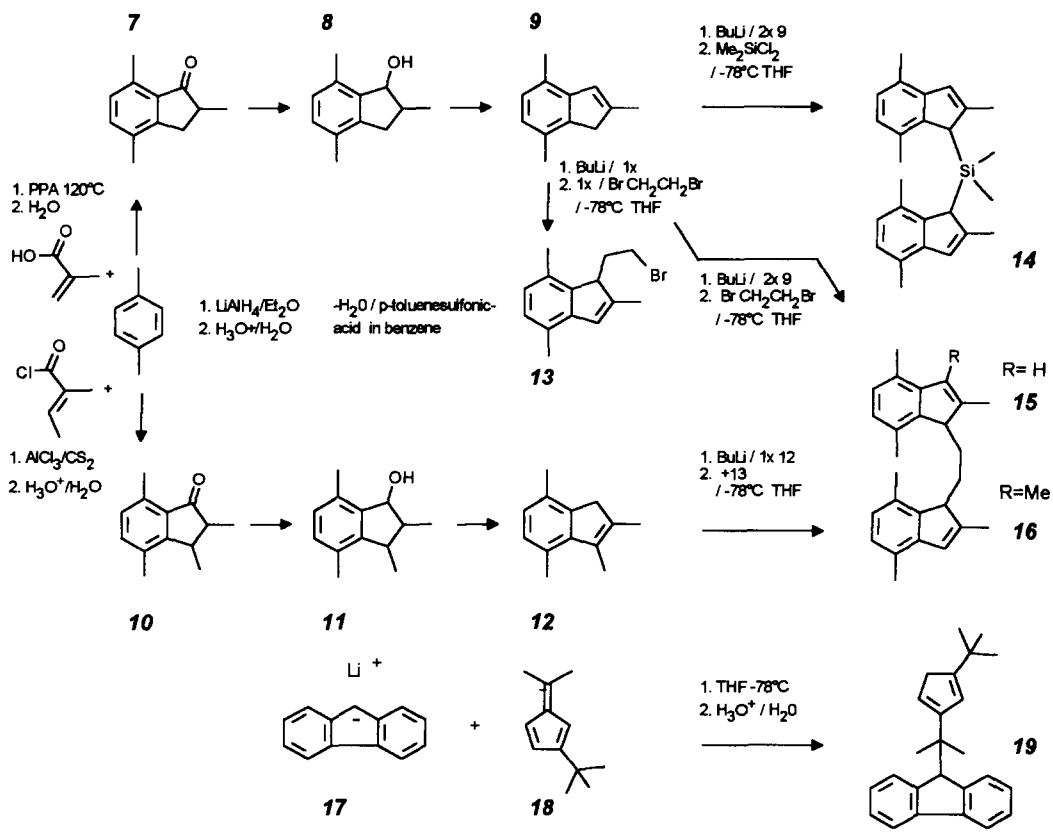

Scheme 1. Synthetic pathway to substituted bridged indene and 2-cyclopentadienyl-2-fluorenylpropane ligands.

separation of *meso* and *rac* forms does not exist for C_s- and C_1-symmetric metallocenes is an advantage of these systems; on the contrary they have so far not reached the excellent polymerization results of the substituted indenyl systems.

2. Results

2.1. Synthesis

A synthesis was designed leading to 2,4,7-trimethylindene and 2,3,4,7-tetramethylindene without the drawback of receiving positional isomers. *p*-Xylene was chosen as a starting material. The synthesis of **10** proceeded well using a Friedel–Crafts acylation–alkylation step according to Hart and Tebbe [16], which has been successfully used for the preparation of indenes [17–20]. Choosing the same synthetic route or applying ethylcyclopropane carboxylate as the Friedel–Crafts agent [21] to receive 2,4,7-trimethylindanone (**7**) led to small yields. Polyphosphoric acid (PPA) is known as a cyclization reagent for unsaturated acids [22] and has been used with α, β unsaturated acids and anisol to give arylvinylketones [23]; cyclization with veratrol led to 2-methyl-5,6-dimethoxymethylindanone [24]. PPA was found to be a successful cyclization reagent in the case of *p*-xylene and methacrylic acid for the large-scale preparation of **7**. The further preparation is straightforward. A general synthetic pathway is outlined in Scheme 1 and described in detail in Section 3. For purification it was found to be important to carry out the metallation steps in a hydrocarbon solvent in order to separate the lithiumindenyl as a white solid powder. 1-(2-Bromoethyl)-2,4,7-trimethylindene (**13**) could be obtained as a crystalline solid when reacting lithiumindenyl with an equimolar amount of dibromoethane in the cold. This valuable new synthetic pathway can be used to prepare bridged unequally substituted bisindenyl ligands (**16**).

The yields for the last step of the synthesis to give the zirconocene were low and resulted in an orange (**2**) or yellow (**4**, **5**) powder, which upon a first crystallization from toluene (**4**, **5**) or CH_2Cl_2 (**2**) yielded a spectroscopically clean product free of any *meso* isomer. Before crystallization no valuable spectra for judging whether any *meso* isomer was present could have been obtained.

2.2. Geometric features

Molecular structures as obtained by X-ray diffraction are reported for **1**, **2**, **4** and **6** in Figs. 1, 2, 3 and 4 respectively. All complexes are pictured in Fig. 5. Some important distances and angles are listed in Table 1.

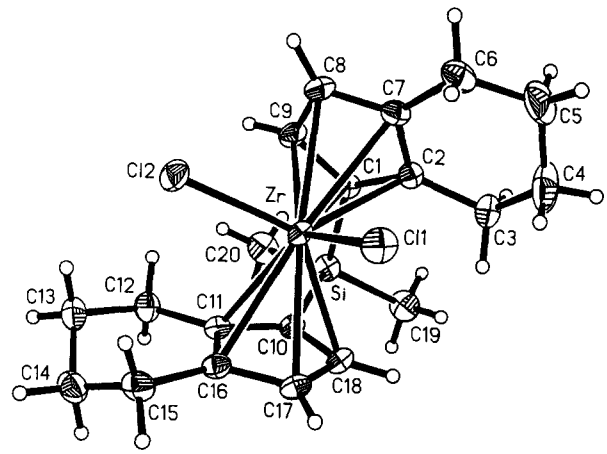

Fig. 1. Molecular structure of **1** at 293 K with 30% probability thermal ellipsoids depicted.

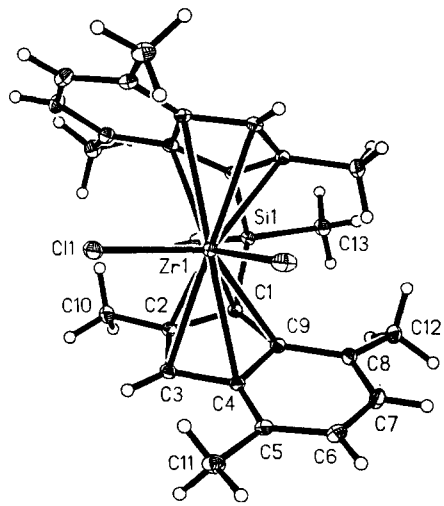

Fig. 2. Molecular structure of **2** at 153 K with 30% probability thermal ellipsoids depicted.

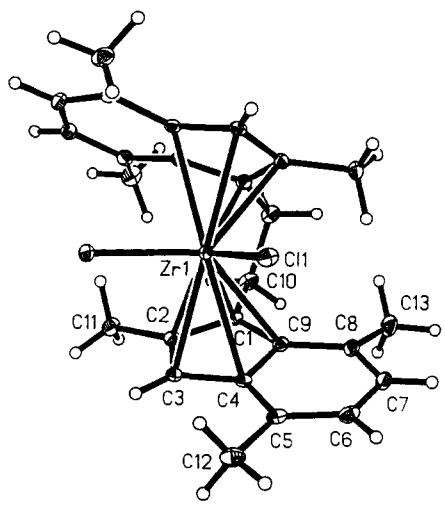

Fig. 3. Molecular structure of **4** at 153 K with 30% probability thermal ellipsoids depicted.

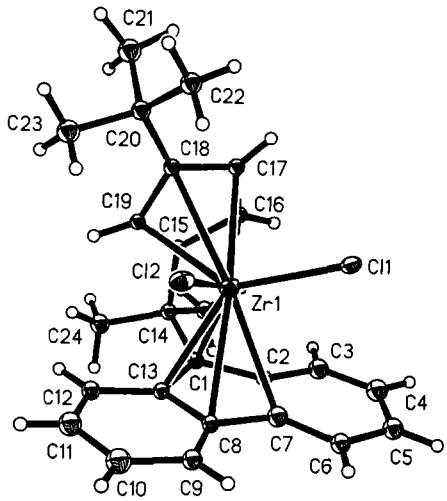

Fig. 4. Molecular structure of **6** at 153 K with 30% probability thermal ellipsoids depicted.

Details of the X-ray measurements and the crystallographic data are given in Section 3.

The following geometric properties are worthwhile mentioning. The bending of the Si–C bonds out of the mean plane of the adjacent C_5 ring for **2** is fairly large (19.1°). For both of the trimethyl-substituted complexes

Table 1
Selected distances (Å) and angles (°)

	1	**2**	**4**	**6**
Distances				
Zr–Cl_1	2.444	2.414	2.434	2.420
Zr–Cl_2	2.440	2.414	2.434	2.420
Zr–ce_1	2.226	2.236	2.232	2.184
Zr–ce_2	2.225	2.236	2.232	2.245
Zr–C_1(bridge)	2.473	2.473	2.497	2.428
Zr–C_2(bridge)	2.483	2.473	2.492	2.420
Angle				
Cl_1–Zr–Cl_2	97.3	97.2	96.3	96.2
ce_1–Zr–ce_2	126.3	129.5	127.6	118.5
Cl_1–Zr–ce_1	107.3	106.1	107.1	110.8
Cl_2–Zr–ce_2	107.6	106.1	107.2	108.8
C_1(bridge)–ce_1–Zr	86.4	85.4	87.3	86.0
C_1(bridge)–ce_2–Zr	86.8	85.4	87.5	82.5
ce_1–C_1(bridge)–X(bridge)	163.3	160.9	177.3	165.2
ce_2–C_2(bridge)–X(bridge)	162.7	160.9	177.4	168.0
Torsion angles				
C_1(bridge)–ce_1–ce_2–C_2(bridge)	2.3	9.2	9.1	0.5
C_1(bridge)–ce_1–Zr–ce_2	6.9	4.0	3.8	0.2
C_2(bridge)–ce_2–Zr–ce_1	4.9	4.0	4.1	0.2

The lower subscript numbers refer to the upper ring (alternatively to the left-hand side) of the compound as displayed in Fig. 5, C(bridge) refers to a C atom of the C_5 ring connected to the bridging group, X(bridge) refers to the C or Si atom in the bridge, and ce refers to the geometric midpoint of the C_5 ring.

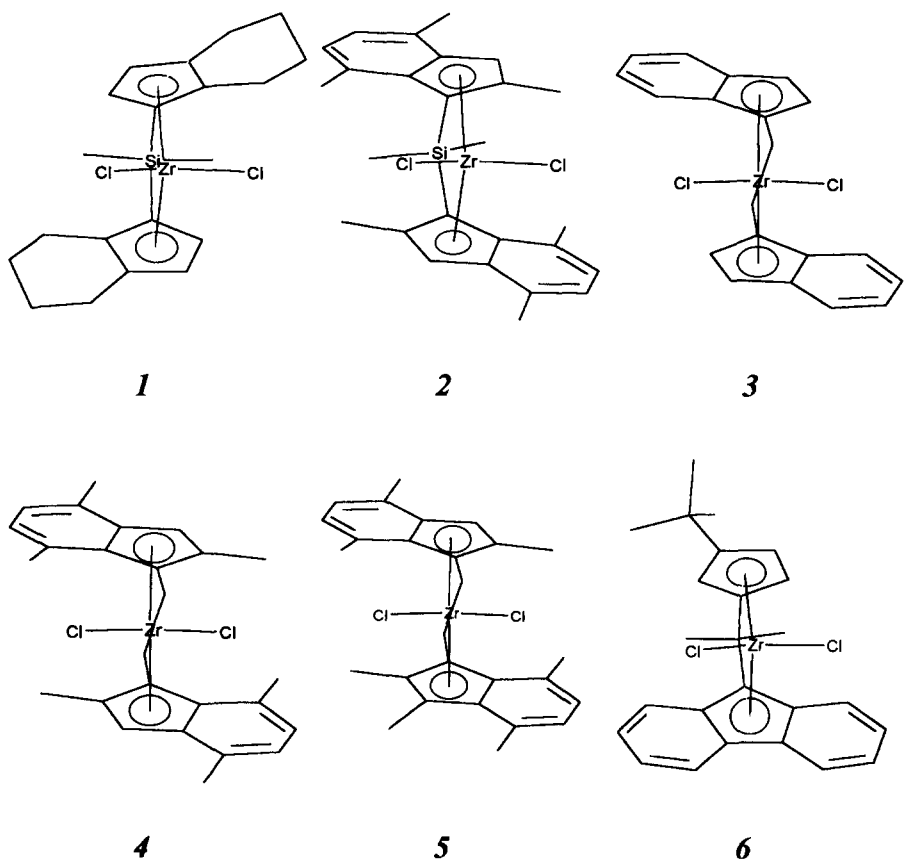

Fig. 5. Structures of the ansa zirconocene dichlorides as discussed in this paper.

Table 2
Comparison of propene polymerization results for methyl-substituted bridged indenyl zirconocene–methylalumoxane catalysts

Bridge	Positions of Me substituent	T_P (°C)	Activity (kg polypropene (mol Zr)$^{-1}$ h^{-1})	M_n (g mol^{-1})	*mmmm* (%)	Differential scanning calorimeter m.p. (°C)	Reference
$-CH_2CH_2-$	3	50	10200	26000	18	No. m.p.	[14]
$-CH_2CH_2-$	4,7	40	32000	16000	79.4	115	[19]
$-CH_2CH_2-$	4,7	50	94200	4000	–	130	[26]
$-CH_2CH_2-$	2,4,7	50	49000	24400	–	152	[26]
$-CH_2CH_2-$	5,6	40	7800	5800	92.2	130	[27]
$(CH_3)_2Si$	2	50	40000	≈ 170000	90.2	148	[5]
$(CH_3)_2Si$	2	50	9200	82300	90	150	[11]
$(CH_3)_2Si$	3	70	33000	28000	≲ 20	–	[4]
$(CH_3)_2Si$	4,7	50	32500	6900	–	134	[26]

Some results vary owing to different experimental conditions.

the two indenyl rings are twisted significantly away from each other by dihedral angles of 9.2° and 9.1° respectively, as a consequence of the steric stress due to the crowded situation at the bridging group. The Zr–centroid (ce) distances are slightly enlarged compared with other ethylidene or dimethylsilyl bridged zirconocenes (see **1** compared with **2** and **4**). Complex **6** is very similar in geometry to its unsubstituted counterpart prepared by Ewen and Razavi [25]. Only the distance from the Zr atom to the C_5-ring-C-atom substituted with the *tert*-butyl group is found to be lengthened by about 0.08 Å; all other distances are identical within 0.02 Å.

2.3. Polymerization behaviour

To investigate and compare the effect of methyl substitution on the catalytic behaviour of **1–6**, polymerizations in the presence of methylalumoxane (MAO) were carried out in liquid propene at various polymerization temperatures. The polymerization results are in agreement with results from literature as reported in Table 2.

Only **2** exhibits much higher molecular weights as expected from a reference in the patent literature. No regiodefects were found in the polymers produced with **2**, **4** and **5** except polypropene obtained from **2** at $T_P = 60$ °C exhibited 0.8% 2,1 insertions of propene units. The low isotacticity of polypropene obtained from **2**–MAO does not correspond to the relatively high melting points observed. It is worthwhile mentioning that the new complex **2** exhibits at $T_p = 30$ °C and $P_{ethene} = 2$ bar a polymerization activity towards ethene which is the highest so far observed. The ethene polymerization activity of 111 900 kg PE (mol Zr)$^{-1}$h^{-1}C$^{-1}_{ethene}$ [28] for **2** exceeds the activity of Cp_2ZrCl–MAO by a factor of almost 2 [29]. Bearing the literature results in mind, one would expect almost total loss of stereospecificity in the 3-position-substituted complexes. Polymerization results of **5**–MAO suggest a comparable degree of stereocontrol as shown for the unsubstituted bisindenyl complex **3**. This is unexpected and cannot be explained if the mechanism of chain migration applies since geometries of the two possible coordination sites differ significantly.

The polymer produced with **6** possesses a rather low melting point although the pentad isotacticity is near to 90% (Table 3). It is interesting to note that the isotacticity remains constant over a wide temperature range. The molecular weights show the usual decline with increasing temperature. In comparison with $[Me_2C(Cp)(Fluo)]ZrCl_2$ a lower activity is found. The change in the microstructure from syndiotactic to isotactic polypropene might be caused by a blocking of chain migration. If the substituent at the Cp ring is reduced in size to a methyl group, chain migration still occurs as

Table 3
Propene bulk polymerization

Catalyst	T_p (°C)	Activity (kg mol^{-1} h^{-1})	M_η (kg mol^{-1})	M.p. (°C)	*mmmm* (%)
1	0	200	147	159	94
	30	4000	45	154	96
	60	65000	21	142	91
2	0	1200	290	158	70
	30	25000	185	154	65
	60	45000	85	147	62
3	0	2500	109	152	95
	30	90000	53	142	93
	60	150000	34	134	90
4	0	1500	1050	165	99
	30	10000	570	163	99
	60	18000	170	160	98
5	30	600	80	158	90
6	30	4000	185	126	88
	60	15700	40	128	88

Polymerization conditions and polymer analyses are outlined in Section 3.

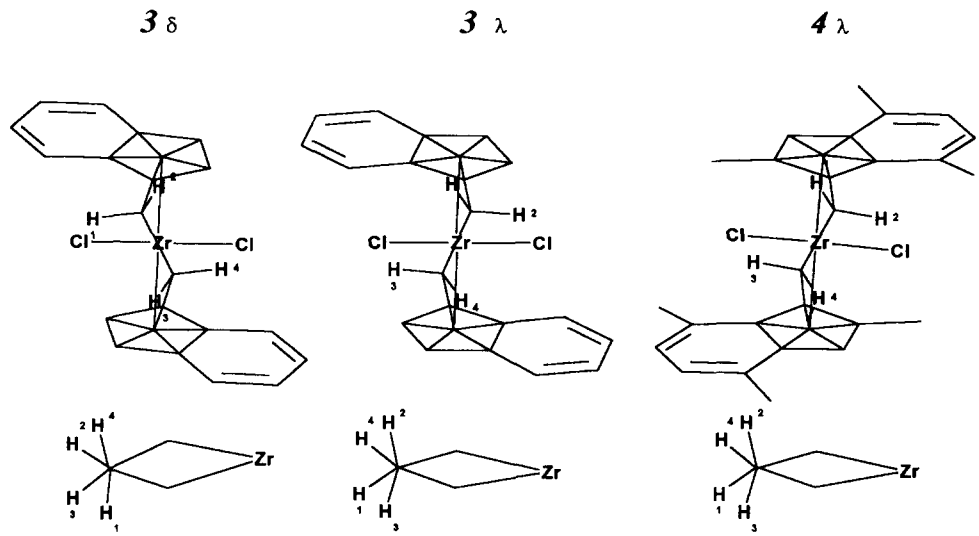

Fig. 6. Positional exchange of the ethylidene protons as determined by NMR measurements.

proven by the generation of hemi-isotactic polypropene [30].

2.4. Dynamic behaviours of 3 and 4

Ethylidene-bridged catalysts are less rigid than one would expect at first sight. The ethylene bridge together with the carbon atoms of the Cp ring and the zirconium atom can be considered as a five-membered ring, having two conformational geometries. Applying the nomenclature of Corey and Bailar [31] and Purcell and Kolz [32], one can assign the symbol δ for right-handed ring helicity and λ for left-handed ring helicity.

If the five-membered ring does a flip–flop the molecule interchanges for example from the δ to the λ states with the result that H(1) and H(4) atoms become equatorial while H(2) and H(3) become axial (Fig. 6). The $^{1}H\,^{3}J$ coupling constants of the ethylene bridge are a good measure of the geometrical conformation of the ring. The AABB spin-coupling system can easily be calculated by means of a computer program [33].

When comparing the geometry in terms of torsion angles with the coupling constants for the H–C–C–H bond of the 1,2-ethylidene bridge (Table 4) only for **4** are the ^{3}J coupling constants in accordance with the torsion angles as expected from the Karplus–Conroy

Table 4
Geometry (angles (°)) and ^{1}H coupling (Hz) in the ethylidene bridge of **3** and **4**, together with the energy (kcal mol^{-1})

	3 δ [a], Calculated	**3** λ [a], Calculated	**4** λ [a], Crystal structure	**3** (δ + λ) [b]	**4** (λ) [b]
	Angle			*$^{1}H\,^{2}J$ coupling*	
H_1–H_2	106.4	106.0	103.9	−14.7	−15.2
H_3–H_4	106.4	106.0	103.9	−14.7	−15.2
	Torsion angle			*$^{1}H\,^{3}J$ coupling*	
H_1–H_3	44.3	38.7	30.1	7.2	8.8
H_2–H_3	72.1	154.8	147.3	7.8	11.9
H_1–H_4	160.7	77.3	87.1	6.8	1
H_2–H_4	44.3	38.7	30.1	7.2	8.8
	Torsion angle				
C(bridge)–ce–ce–C(bridge)	18.3	13.4	9.1		
C(bridge)–ce–Zr–ce	8.1	5.9	3.8		
C(bridge)–ce–Zr–ce	8.1	5.9	4.1		
	Energy (MM calculated)				
Total potential energy	11.5	11.3	15.8		

[a] Geometric features of **3** and **4**.

[b] Calculated ^{1}H NMR (360 MHz) coupling. Shifts in $CDCl_2$–$CDCl_2$ for **3**: H_{2+3}, 3.793 ppm; H_{1+4}, 3.755 ppm; $W_{1/2}$ = 1.0 Hz for **4**: H_{2+3}, 3.922 ppm; H_{1+4}, 3.705 ppm; $W_{1/2}$ = 1.0 Hz.

equation. It must be concluded that, in the case of **3**, none of the two conformers exists exclusively at the NMR recording temperature of 311 K (Fig. 7). The exchange of the methylene protons between the equatorial and axial positions leads to an averaging of the coupling constants.

Temperature-dependent dynamic NMR measurements reveal that exchange occurs within the time scale of NMR measurements (Fig. 8). The rate constant of the flip–flop can be enhanced with temperature, leading to coalescence of the signals.

Molecular mechanics (MM) calculations were performed on **3** and **4** using the force field program Discover 2.9 [34] and a modified cff91 valence force field [35]. Forcing the zirconium–centroid torsion angles to adopt certain angles with a high force constant (1000 kcal mol^{-1}) while minimizing the rest of the molecule results in the two-dimensional energy maps of the conformational flexibility as displayed in Fig. 9. The energy map for **3** reveals the existence of two conformational states with a low transition barrier as confirmed by the NMR experiments. A second minimum for a δ ring helicity cannot be detected for **4**.

The horizontal extension of the minima can be taken as a measure of the ease with which chlorine atoms adopt certain positions along the so-called "lateral extension angle" [37] (Fig. 10). This model can be employed for alkyl–olefin complexes to describe the conformational space available to the olefin and alkyl groups. It has been stated that the transition states for β-H elimination via transfer to the metal centre or transfer to the olefin causing a chain termination are sterically more demanding than is the actual olefin insertion process [11]. Experimental results exhibit higher molecular weights for **4**, thus confirming the theoretical approach derived from the metallocene dichlorides of **3** and **4**.

MM calculations have been performed with **3** and **4**; instead of the chlorides a π-coordinated propene and an isobutyl fragment were used as ligands. If the olefin is coordinated suitably for a 1,2 insertion, the value of the total potential energy $\Delta(re\text{–}si$ coordination of the olefin) is more in favour of *mm* enchainments in the case of **4** [37]. Potential energy values $\Delta(re\text{–}si)$ are calculated for all rotational states of the ce(olefin)–Zr–C_α–C_β-torsion angle in incremental 5° steps with a force constant of 1000 kcal mol^{-1}. No other restraints have been employed. The olefin is unstrained and remains in a favourable position for 1,2 insertion. The experimental increase in isotacticity of the polymer produced by **4** compared with **3** is in agreement with MM calculations. The stereochemistry of the 2,1 insertion is not yet comprehensible with the selected MM approach.

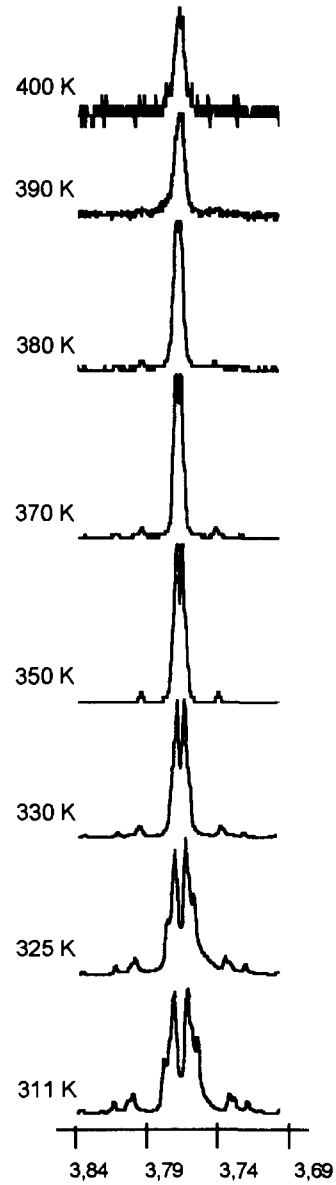

Fig. 8. Temperature dependent ^1H NMR (360 MHz) (ppm) of the methylene region of **3**.

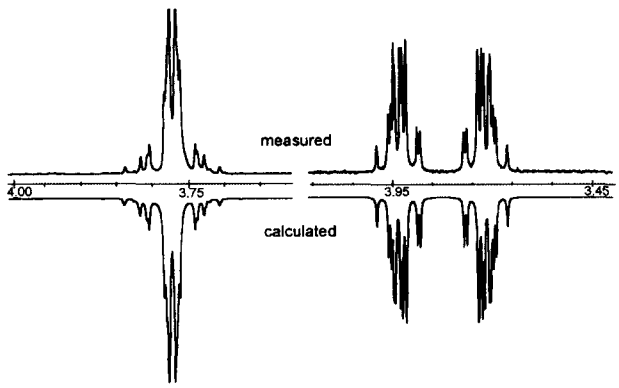

Fig. 7. ^1H NMR (360 MHz) (ppm): methylene region of (a) **3** at 311 K and (b) **4** at 340 K.

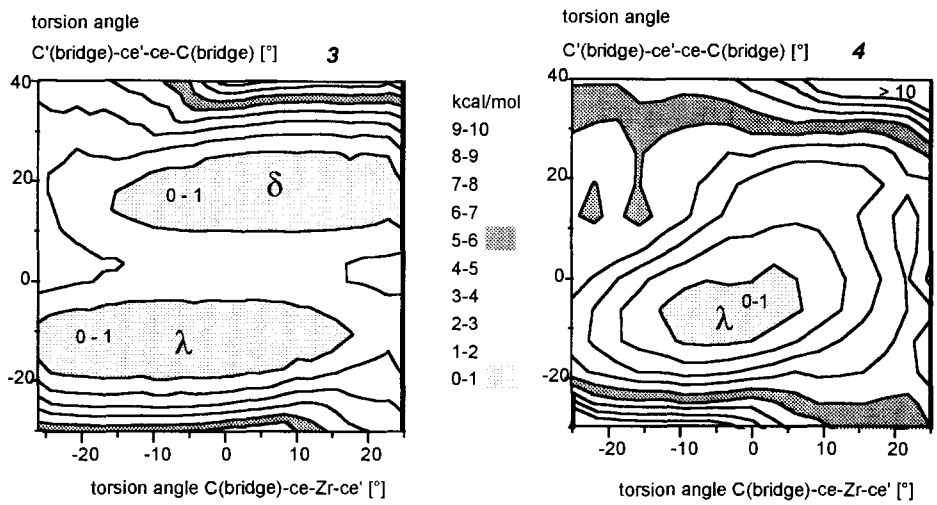

Fig. 9. Flexible-geometry contour map of the total potential energy above the minimum conformation (see Table 4) of (a) **3** and (b) **4** calculated by relaxing the entire molecule while systematically sampling the torsion angles C(bridge)–ce–Zr–ce' and C'(bridge)–ce'–Zr–ce, which were restrained with 1000 kcal mol^{-1}. The energy is contoured in 1 kcal mol^{-1} intervals as a function of C(bridge)–ce–Zr–ce' and C'(bridge)–ce'–ce–C(bridge) torsion angles. ce refers to the centroid of the five-membered ring, and C(bridge) to the carbon atom of the five-membered ring substituted with the bridging group.

3. Experimental section

3.1. General comments

Synthetic procedures were performed under an atmosphere of argon using Schlenk techniques. Non-halogen solvents were distilled from sodium–potassium prior to use. Dichloromethane was refluxed with calcium hydride and finally distilled from sodium–lead. ^1H NMR spectra were recorded on a Bruker AC 100 spectrometer, a Bruker MSL 300 spectrometer and a Bruker AM 360; IR spectra were recorded on a Nicolet FT-IR SXB spectrometer, and mass spectra on a VG 70VSE mass spectrometer.

3.2. Polymerization procedures

Polymerization grade propene was purchased from Gerling, Holz & Co and purified by passage through columns with Cu catalyst (BASF R3-11) and a molecular sieve of 10 Å. MAO was used as a 10 wt.% solution in toluene (cryoscopic $M = 1340$ g mol^{-1} (benzene); [Me]/[Al] = 1.66). Polymerizations were performed in a Büchi AG type IV 11 steel autoclave. For a typical polymerization, 350 ml of propene were condensed into the autoclave. Each 3 ml of MAO solution were added into the propene and reacted separately with an appropriate amount of metallocene to yield 5–10 g of polypropene. The catalyst was added to the autoclave after 15 min. A high level of temperature constancy was achieved with a Büchi data system 488 and two thermostats. Polymerization was stopped after 1 h by the addition of ethanol. Propene pressure was released and the product removed from the autoclave, washed with ethanol–HCl, neutralized and dried in vacuum.

3.3. Polymer analyses

Viscosimetry was carried out with an Ubbelohde capillary 0a ($K = 0.005$) at 135 °C using decahydronaphthalene as solvent. The Mark–Houwink constants ($k = 0.0238$ mlg^{-1}; $a = 0.725$) have been reported in the literature [38]. Molecular weight distributions were determined by gel permeation chromatography on a Waters 150-C instrument. All samples showed molecular weight distributions M_W/M_N below 2.7. Differential scanning calorimetry analyses were performed on a Perkin–Elmer DSC-4 instrument (heating rate, 20 °C

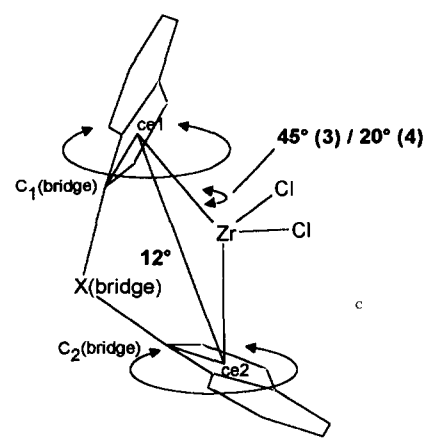

Fig. 10. Rotational freedom in the 1 kcal mol^{-1} total potential energy minima of **3** and **4**.

min^{-1}). The minima of the second scan are reported. For polymer ^{13}C NMR spectra a 250 mg polymer sample, 2 ml of hexachlorobutadiene and 0.25 ml of tetrachloroethane-d_2 were dissolved by heating in a 10 mm NMR tube. Spectra were recorded at 100 °C on a 300 MHz Bruker MSL 300 spectrometer. The percentage of the *mmmm* pentads was determined with the deconvolution routine of the Bruker WIN-NMR program.

3.4. Preparation of 2,4,7-trimethylindanone (7)

In a three-necked flask equipped with a mechanical stirrer, a dropping funnel and a reflux condenser, 145 ml (1.18 mol) of xylene and 900 g of PPA were rapidly stirred and heated to 120 °C. When phase mixing had occurred, 120 ml (1.18 mol) of methacrylic acid were added slowly through the dropping funnel. Heating was continued for another 50 min, followed by cooling to room temperature and quenching with ice–water. Extraction with three portions of each 300 ml of diethyl ether, working up the combined ether fractions in the usual manner with water, water–$NaHCO_3$ and drying with $NaSO_4$ afforded after distillation under high vacuum (fraction at 110–125 °C) a yellow oil. The oil was crystallized from methanol at −18 °C resulting in 52 g (30%) of a crystalline product (white needles) (melting point (m.p.), 35 °C). IR (NaCl): ν 2963, 2923, 2871, 1705, 1587, 1496, 1457, 1437, 1248, 966, 820 cm^{-1}. ^1H NMR ($CDCl_3$ 100 MHz): δ 7.20 (d, 1H, $^3J = 7.5$ Hz), 6.97 (d, 1H, $^3J = 7.5$ Hz), 3.12 (dd, 1H, $^3J = 8$ Hz), 2.6–2.3 (m, 2H), 2.57 (s, 3H), 2.25 (s, 3H), 1.27 (d, 3H, $^3J = 7.3$ Hz) ppm.

3.5. Preparation of 2,4,7-trimethylindanol (8)

88.75 g of indanone (0.51 mol) in 100 ml of diethyl ether were added through a dropping funnel to 500 ml of diethyl ether and 7.9 g (0.21 mol) of $LiAlH_4$. Refluxing for 3 h and quenching with 10 ml each of ice–water, aqueous NaOH solution and water afforded after ether extraction and work-up of the combined organic layers a white product which could be crystallized from PE 60/70 at room temperature (yield, 78.4 g (87%); m.p., 93 °C). IR (NaCl): ν 3289, 2957, 2925, 2897, 2867, 1489, 1456, 1330, 1071, 1042, 808 cm^{-1}. ^1H NMR ($CDCl_3$, 100 MHz): δ 7.06 (d, 1H, $^3J = 8.5$ Hz), 6.90 (d, 1H, $^3J = 8.9$ Hz), 4.82 (m, 1H), 3.08 (m, 1H), 2.37 (s, 3H), 2.27 (d, 2H, $^3J = 5.6$ Hz), 2.19 (s, 3H), 1.53 ((–OH) d, 1H, $^3J = 7.3$ Hz), *exo–endo* isomer 1,12; 1.23 (d, 3H, $^3J = 6.8$ Hz; $^3J = 6.6$ Hz) ppm.

3.6. Preparation of 2,4,7-trimethylindene (9)

300 ml of Benzene, 82.4 g of trimethylindanol, 1 g of p-toluenesulphonic acid and a few crystals of 2,6-di-*tert*-butyl-3-methyl-phenol were refluxed for 35 min until 8.2 ml of water had been collected in a water separating funnel. The product was washed with water–NH_4Cl and dried over Na_2SO_4. Removal of the solvent crystallization from ethanol yielded 65.7 g (88.7%) of a white product (m.p., 42 °C). IR (NaCl): ν 3040, 2960, 2915, 2875, 1496, 1440, 1387, 1021, 901, 825, 799 cm^{-1}. ^1H NMR ($CDCl_3$, 100 MHz): δ 6.99 (d, 1H, $^3J = 7.7$ Hz), 6.84 (d, 1H, $^3J = 7.7$ Hz), 6.68 (q, 1H, $^4J = 1.5$ Hz), 3.20 (s, 2H), 2.38 (s, 3H), 2.31 (s, 3H), 2.19 (s, 3H) ppm.

3.7. Preparation of 2,3,4,7-tetramethylindanone (10)

To 27.2 g of tiglic acid chloride and 25.8 g of *p*-xylene in 250 ml of dry CS_2 were added 33 g of $AlCl_3$ in small portions. Stirring by a mechanical stirrer for $\frac{1}{2}$ h was followed by refluxing for 1 h. After cooling, the red viscous solution was poured over 800 g of ice and 600 ml of concentrated HCl. The organic layer was separated and the residue extracted twice with diethyl ether. The ether phase was washed with water and dried over Na_2SO_4. Distillation at 4 mbar and 95°C afforded 21 g (48% yield) of the product as a colourless oil. IR (NaCl): ν 1700 cm^{-1}. ^1H NMR ($CDCl_3$, 100 MHz); δ 7.03 (d, 1H, $^3J = 7.5$ Hz), 6.80 (d, 1H, $^3J = 7.6$ Hz), 3.28 (m, 1H), 2.71 (m, 1H), 2.43 (s, 3H), 2.18 (s, 3H), 1.25–0.9 (*exo–endo* isomers, 6H) ppm.

3.8. Preparation of 2,3,4,7-tetramethylindanol (11)

Following the procedure described for **8**, 21 g of tetramethylindanore in 100 ml diethyl ether were added to 2.4 g (0.06 mol) of $LiAlH_4$ in 350 ml of diethyl ether to yield 19.1 g (91%) of a colourless solid. IR (NaCl): ν 3340, 2956, 2901, 2869, 1490, 1440, 1370, 788 cm^{-1}.

3.9. Preparation of 2,3,4,7-tetramethylindene (12)

Following the procedure as described for **9**, 19.1 g (0.1 mol) of 2,3,4,7-tetramethylindanol were refluxed in benzene. The product was isolated as the fraction boiling at 135°C and 3 mbar. Recrystallization from ethanol yielded 13.5 g (78%) of slightly yellow crystals. IR (NaCl): ν 2955, 2909, 2869, 1490, 1445, 1377, 1150, 1025, 792 cm^{-1}. ^1H NMR ($CDCl_3$, 100 MHz): δ 6.97 (d, 1H, $^3J = 8$ Hz), 6.84 (d, 1H, $^3J = 8$ Hz), 3.15 (s, 2H), 2.60 (s, 3H), 2.31 (s, 3H), 2.26 (s, 3H), 2.1 (s, 3H) ppm.

3.10. Preparation of 1,2-bis(2,4,7-trimethylindene) ethane (15)

To 19 g (0.12 mol) of trimethylindene dissolved in 300 ml of dry pentane, 50 ml of 2.5 M *n*-butyllithium solution in hexane were added through a dropping funnel. A white voluminous solid precipitated. Stirring

was continued for 5 h, after heating the suspension to boiling the solid was collected in a D4 glass frit and washed with 50 ml of pentane. After drying, 19.6 g (99%) of a white powder were obtained. To 200 ml of tetrahydrofuran (THF) at −78°C the lithiumtrimethylindenyl powder (0.12 mol, 19.6 g) was added; thereafter 11.3 g (0.06 mol) of dibromoethane were added at once. The yellow solution turned to red, indicating complete reaction. After stirring for 12 h at room temperature, 2 ml of water were used for quenching followed by an aqueous work-up and extraction with diethyl ether. After drying the diethyl ether solution over $NaSO_4$, the solvent was removed and the product crystallized from ethanol–diethyl ether (2:1) affording 11 g (54%) of a white light powder (m.p., 210°C). IR (KBr solid): ν 3043, 2950, 2917, 2869, 1647, 1487, 1436, 1380, 857, 800 cm^{-1}. ^1H NMR ($CDCl_3$, 100 MHz): δ 6.93 (d, 2H, $^3J = 7.7$ Hz), 6.73 (d, 2H, $^3J = 7.7$ Hz), 6.54 (s, 2H), 3.18 (s, 2H), 2.34 (s, 6H), 2.00 (s, 6H), 1.92 (s, 6H), 1.33 (s, 4H) ppm. Mass spectroscopy (MS): *m/z* (relative peak height (%)): 342 (35) M^+, 184 (15), 170 (100), 156 (22), 141 (18), 128 (10).

3.11. Preparation of 1-(2,4,7 trimethylindene)-2-bromoethane (13)

Following the procedure described for **15**, lithiumtrimethylindene was reacted with equimolar amounts of dibromoethane in 200 ml of THF, kept at −78°C for 5 h and slowly warmed to room temperature. Crystallization from ethanol–diethyl ether (4:1) yielded 15.9 g (94%) of a white grainy powder (turning yellow after 2 days). IR (NaCl): ν 3039, 2960, 2906, 2861, 1493, 1443, 1376, 1232, 860, 802 cm^{-1}. ^1H NMR ($CDCl_3$, 100 MHz): δ 6.95 (d, 1H, $^3J = 7.7$ Hz), 6.80 (d, 2H, $^3J = 7.7$ Hz), 6.57 (s, 1H), 3.46 (m, 1H), 2.8–2.4 (m, 4H), 2.38 (s, 3H), 2.32 (s, 3H), 2.03 (s, 3H) ppm. MS:*m/z* (relative peak height (%)):266 (50), 264(51) M^+, 185(15), 171 (100), 157 (92), 141 (33).

3.12. Preparation of 1-(2,4,7-trimethylindene)-2-(2,3,5,7-tetramethylindene)ethane (16)

The lithium salt of tetramethylindene was prepared as described above (yield, 8.7 g, 0.049 mol (86%)). Following the procedure described for **15** the powder was added to 250 ml of THF at −78°C containing **13**. After 12 h the solution was heated to boiling to dissolve the product completely. After removal of the solvent the product was precipitated from hot EtOH–diethyl ether and recrystallized from THF–PE 60/70 (1:2) to yield 4.2 g (48%) of a white powder (m.p., 242°C). ^1H NMR ($CDCl_3$, 100 MHz): δ 6.84 (d, 2H, $^3J = 7$ Hz), 6.72 (d, 2H, $^3J = 7.5$ Hz), 6.54 (s, 1H), 3.14 (s, 1H), 3.09 (s, 1H), 2.55 (s, 3H), 2.34 (s, 3H), 2.23 (s, 6H), 1.99 (s, 3H), 1.91 (s, 6H), 1.28 (m, 4H) ppm. MS:*m/z* (relative peak height (%)) 356 (40) M^+, 199 (10), 184 (90), 170 (100), 156 (35), 141 (28).

3.13. Preparation of dimethylsilylbis(2,4,7-trimethylindene) (14)

Following the procedure described for **15**, 20 g (0.12 mol) of trimethylindenyllithium salt were added to 7.9 g (0.06 mol) of dimethylsilyl chloride in dry THF (−78°C) and stirred for 24 h. The work-up is as described above. The product can be crystallized from THF–PE (1:5) (yield, 6.7 g (30%); m.p., 148°C). IR (KBr solid): ν 2959, 2913, 2859, 1495, 1440, 1371, 1243, 1039, 1005, 838, 812, 802 cm^{-1}. ^1H NMR ($CDCl_3$, 100 MHz): δ 6.90 (d, 2H, $^3J = 7.7$ Hz), 6.76 (d, 2H, $^3J = 7.5$ Hz), 6.64 (s, 2H), 3.83 (s, 2H), 2.35 (s, 12H), 2.27 (s, 6H), −0.46 (s, 6H) ppm. MS: *m/z* (relative peak height (%)) 372 (13) M^+, 215 (100), 157 (10), 155 (9).

3.14. Preparation of 2-(3-tert-butyl(cyclopentadienyl)-2-fluorenylpropane (19)

tert-Butylcyclopentadiene was prepared from cyclopentadiene magnesium bromide and *tert*-butyl chloride [39]. Reaction of *tert*-butylcyclopentadiene with acetone in methanol–pyrrolidine led to the formation of 2-*tert*-butyl-6,6-dimethylfulvene (**18**) [40]. The synthesis of **19** was carried out in a 500 ml three-necked flask equipped with stirrer and dropping funnel. 13.30 g (80 mmol) of fluorene were dissolved in 250 ml of THF and cooled to −78°C. 32 ml (80 mmol) of a 2.5 M solution of *n*-butyllithium in hexane were added dropwise; the mixture was slowly warmed to room temperature and again cooled to −78°C. A solution of 12.98 g (80 mmol) of **18** in 50 ml of THF was added slowly into the flask, the reaction mixture warmed to room temperature and hydrolysed with 100 ml of water. Hydrochloric acid was added until acidic reaction, the phases separated and the aqueous layer extracted three times with each 100 ml diethyl ether. The combined organic fractions were washed and dried as described previously and all solvents were removed. The remaining yellow oil was crystallized from diethyl ether–ethanol to yield 20.24 g (77%) of fine white crystals. ^1H NMR ($CDCl_3$, 100 MHz): δ 7.00–7.73 (m, 8H), 6.08 (s, 1H), 5.95 (s, 1H), 4.05 (s, 1H), 3.12 (s, 2H), 1.19 (s, 9H), 1.05 (s, 6H).

3.15. Preparation of dimethylsilylbis(4,5,6,7-tetrahydroindenyl)zirconium dichloride (1)

6.33 g (14.1 mmol) of *rac*-[dimethylsilylbis(indenyl)]zirconium dichloride were dissolved in 500 ml of dichloromethane in a 1 l steel autoclave. Two spatula tipfulls of platinum(IV) oxide hydrate were added and a hydrogen pressure of 17 bar applied. The mixture was

stirred for 3 h at room temperature and filtered through a D 4 frit after release of hydrogen pressure. The filtrate was evaporated to dryness and the residue recrystallized from toluene at 70°C to yield 2.06 g (32%) of **1**. *rac*-[Dimethylsilylbis(indenyl)]zirconium dichloride was prepared according to [3]. ^{1}H NMR ($CDCl_3$, 100 MHz): δ 6.63 (d, 2H), 5.47 (d, 2H), 3.17–2.10 (m, 8H), 2.10–1.16 (m, 8H), 0.74 (s, 6H) ppm.

3.16. Preparation of dimethylsilylbis(2,4,7-trimethylindenyl)zirconium dichloride (2)

Following the procedure as described for **4**, 11.5 g (0.031 mol) of **14** were reacted with butyllithium to give 11.5 g (0.03 mol) of lithium salt powder. The salt was added to 7.1 g of (0.0305 mol) $ZrCl_4$ in $CHCl_2$ at −78°C to give 8 g as a product. Continuous extraction with hot toluene over 4 h yielded 2 g of orange powder. Complete purification was achieved by dissolving 2 g in boiling CH_2Cl_2 (200 ml) and precipitation at −18°C (yield 1 g (6%)). Crystals suitable for X-ray diffraction were grown as described above from hot toluene. IR (KBr solid): ν 3028, 2969, 2936, 1463, 1434, 1293, 1264, 838(s), 819(s), 697, 467 cm^{-1}. ^{1}H NMR ($CDCl_3$, 100 MHz): δ 7.01 (d, 2H, ^3J = 7.0 Hz), 6.81 (d, 2H, ^3J = 6.8 Hz), 6.91 (s, 2H), 2.53 (s, 6H), 2.31 (s, 6H), 2.18 (s, 6H), 1.28 (s, 6H) ppm. ^{13}C NMR ($CdCl_3$, 360 MHz): δ 133.4, 133.1, 132.4, 131.2, 129.5, 123.5, 118.7, 115.3, 87.0, 19.6, 19.1, 18.2, 8.1 ppm. MS:*m/z* (relative peak height (%)) 532 (M^+, 17), 517 ($M^+ - CH_3$, 5), 479 ($M^+ - CH_3 - HCl$, 10), 215 (45), 49 (100).

3.17. Preparation of 1,2-ethylidenebis(2,4,7-trimethylindenyl)zirconium dichloride (4)

6 g (0.0175 mol) of ethylidenebis(trimethylindene) were dissolved in 400 ml of methylcyclohexane at 50°C. While stirring heavily 14 ml (0.038 mol) of 2.5 M butyllithium–hexane solution were added dropwise. Immediately a white voluminous precipitate was formed. Stirring was continued for 5 h; filtration over a D4 Schlenk frit, washing with pentane and drying yielded a white powder (5.8 g, 0.0164 mol). The powder was added at once to a solution of $ZrCl_4 \cdot 2THF$ in 200 ml of THF at −78°C. After warming up to room temperature, THF was condensed off from the yellow solution–suspension, the remaining solid was washed with pentane–toluene (1 : 1) and dried (yield, 5.7 g, 0.0113 mol (65%)) to give a yellow powder. The crude product was dissolved for further purification in 1.5 l of toluene at 90°C and crystallized after hot filtration as a microcrystalline solid (yield, 2.8 g (31%)). Only after a second crystallization procedure as described above with a temperature-controlled cooling to room temperature over 2 days were formed crystals suitable for X-ray diffraction. IR (KBr solid): ν 2963, 2933, 1496, 1449, 1378, 827(s) cm^{-1}. ^{1}H NMR ($CDCl_3$, 100 MHz): δ 6.96 (d, 2H, ^3J = 7.1 Hz), 6.81 (d, 2H, ^3J = 7.1 Hz), 6.41 (s, 2H), 3.82 (m, 4H), 2.89 (s, 6H), 2.23 (s, 6H), 2.11 (s, 6H) ppm. ^{13}C NMR ($CDCl_3$, 360 MHz): δ 140.0, 133.2, 131.8, 129.4, 129.2, 127.9, 125.4, 119.6, 112.5, 31.8, 20.5, 18.7, 14.6 ppm. MS: *m/z* (relative peak height (%)) 502 (M^+, 45), 466 (-HCl, 5), 332 (100), 170 (81).

3.18. Preparation of 1,2-ethylidene-(2,4,7-trimethylindenyl),(2,3,4,7-tetramethylindenyl)zirconium dichloride (5)

The analogous reaction of 3.65 g (0.0103 mol) of the ligand with butyllithium to 3 g (0.0082 mol) of the lithium salt afforded after reaction with 2 g (0.0086 mol) of $ZrCl_4$ 4.1 g of product. Hot extraction from toluene afforded 1.5 g of a yellow powder (28%). Owing to the low solubility in all common solvents no suitable ^{1}H NMR could be received. A complete purification did not succeed. MS:*m/z* (relative peak height (%)) 516 (M^+, 8), 501 (-CH_3, 8), 410 (16), 480 (-HCl, 3), 356 (100).

3.19. Preparation of isopropyliden((3-tert-butyl)cyclopentadienyl-9-fluorenyl)zirconium dichloride (6)

4.93 g (15 mmol) of **19** were dissolved in 120 ml of THF in a 250 ml flask equipped with magnetic stirrer and dropping funnel. The solution was cooled to −78°C; 12 ml (30 mmol) of a 2.5 M solution of *n*-butyllithium in hexane were added dropwise and the solution slowly warmed to room temperature. The solvents were evaporated and the remaining deep-red viscous residue suspended in 150 ml of pentane. A suspension of 3.50 g (15 mmol) of zirconium tetrachloride in 80 ml of pentane was added, the mixture stirred for 3 days at room temperature and the pentane removed. 125 ml of dichloromethane were added, the mixture filtered and half of the solvent evaporated. 3.75 g (51%) of red crystals precipitated from the solution at −18°C. Crystals suitable for X-ray diffraction were grown from dichloromethane slightly above room temperature. ^{1}H NMR ($CDCl_3$, 100 MHz): δ 8.06–8.15 (2t, 2H), 7.74–7.88 (2d, 2H), 7.46–7.61 (t, 2H), 7.15–7.32 (4t, 2H), 6.15 (t, 1H), 5.75 (t, 1H), 5.59 (t, 1H), 2.36 (s, 6H), 1.16 (s, 9H) ppm. Anal. Found: C, 61.26; H, 5.32; Cl, 14.10. $C_{25}H_{26}ZrCl_2$ Calc.: C, 61.46; H, 5.36; Cl, 14.51.

3.20. X-ray structure of 1 [41]

Crystal data: $C_{20}H_{26}Cl_2SiZr$; crystal size, 0.6 × 0.5 × 0.4 mm; monoclinic; space group, $P2_1/c$; tempera-

Table 5
Fractional atomic coordinates and equivalent isotropic thermal parameters with estimated standard deviations for the compound $C_{20}H_{26}Cl_2SiZr$

Atom	x	y	z	U_{eq} (Å^2)
Zr	0.82224(2)	0.86732(1)	0.18122(2)	0.0271(1)
Cl(1)	0.75629(7)	0.72536(3)	0.18881(6)	0.0478(2)
Cl(2)	1.02108(6)	0.84603(5)	0.08122(6)	0.0492(2)
Si	0.70885(6)	1.04667(4)	0.26510(6)	0.0349(2)
C(1)	0.6821(2)	0.9849(1)	0.1290(2)	0.0323(4)
C(2)	0.5994(2)	0.9156(1)	0.1142(2)	0.0336(4)
C(3)	0.4789(2)	0.8968(2)	0.1763(3)	0.0462(6)
C(4)	0.4215(4)	0.8166(3)	0.1385(5)	0.0861(9)
C(5)	0.4287(4)	0.7981(3)	0.0141(4)	0.0822(9)
C(6)	0.5626(3)	0.7979(2)	−0.0318(3)	0.0506(6)
C(7)	0.6379(3)	0.8695(1)	0.0163(2)	0.0379(5)
C(8)	0.7465(3)	0.9066(2)	−0.0272(2)	0.0408(5)
C(9)	0.7747(2)	0.9770(1)	0.0413(2)	0.0380(5)
C(10)	0.8150(2)	0.9690(1)	0.3401(2)	0.0304(4)
C(11)	0.9487(2)	0.9568(1)	0.3281(2)	0.0305(4)
C(12)	1.0490(2)	1.0180(2)	0.2974(3)	0.0417(5)
C(13)	1.1821(2)	0.9799(2)	0.2921(3)	0.0498(6)
C(14)	1.2085(3)	0.9174(2)	0.3879(3)	0.0520(7)
C(15)	1.1157(3)	0.8455(2)	0.3763(2)	0.0451(6)
C(16)	0.9806(2)	0.8763(1)	0.3667(2)	0.0340(4)
C(17)	0.8681(2)	0.8380(2)	0.3995(2)	0.0375(5)
C(18)	0.7663(2)	0.8937(1)	0.3828(2)	0.0348(4)
C(19)	0.5602(3)	1.0645(2)	0.3449(3)	0.0544(7)
C(20)	0.7917(3)	1.1446(2)	0.2380(3)	0.0546(8)

ture, 293 K; $a = 1045.4(2)$, $b = 1646.6(3)$ and $c = 1141.9(2)$ pm; $\beta = 92.73(3)°$; $V = 1963.4(6) \times 10^6$ pm^3; $Z = 4$; $d_{calc} = 1.545$ g cm^{-3}; linear absorption coefficient $\mu = 0.893$ mm^{-1} (Mo Kα); 5717 independent reflections; $2\theta_{max} = 60.0°$; number of parameters, 244; final R value, 0.046 (all reflections); program, SHELXL-93 [42].

Table 6
Fractional atomic coordinates and equivalent isotropic thermal parameters with estimated standard deviations for the compound $C_{26}H_{30}Cl_2SiZr$

Atom	x	y	z	U_{eq} (Å^2)
Zr(1)	0.5000	0.73933(2)	0.2500	0.01279(7)
Cl(1)	0.62567(5)	0.62679(4)	0.17803(4)	0.0275(1)
Si(1)	0.5000	0.97240(5)	0.2500	0.0151(1)
C(1)	0.5627(2)	0.88278(12)	0.33936(12)	0.0150(3)
C(2)	0.6658(2)	0.83245(13)	0.31565(12)	0.0157(3)
C(3)	0.6736(2)	0.74806(13)	0.36844(12)	0.0166(3)
C(4)	0.5811(2)	0.74285(12)	0.43074(12)	0.0155(3)
C(5)	0.5563(2)	0.67146(13)	0.49872(13)	0.0184(3)
C(6)	0.4645(2)	0.68661(14)	0.55434(14)	0.0228(4)
C(7)	0.4003(2)	0.77101(14)	0.54576(14)	0.0224(4)
C(8)	0.4211(2)	0.84100(13)	0.48014(13)	0.0184(3)
C(9)	0.5128(2)	0.82658(12)	0.41578(12)	0.0154(3)
C(10)	0.7583(2)	0.86058(15)	0.24934(15)	0.0218(4)
C(11)	0.6268(2)	0.58383(14)	0.50318(15)	0.0250(4)
C(12)	0.3561(2)	0.93150(14)	0.48791(14)	0.0224(4)
C(13)	0.3914(2)	1.05781(14)	0.29152(15)	0.0231(4)

Table 7
Fractional atomic coordinates and equivalent isotropic thermal parameters with estimated standard deviations for the compound $C_{26}H_{28}Cl_2Zr$

Atom	x	y	z	U_{eq} (Å^2)
Zr(1)	0.0000	0.29668(3)	0.2500	0.01227(7)
Cl(1)	0.09921(2)	0.10162(5)	0.27723(3)	0.0210(1)
C(1)	0.0103(1)	0.5433(2)	0.1540(1)	0.0171(3)
C(2)	−0.0447(1)	0.4433(2)	0.1106(1)	0.0182(3)
C(3)	−0.0096(1)	0.3039(2)	0.0781(1)	0.0179(3)
C(4)	0.0684(1)	0.3175(2)	0.0961(1)	0.0160(3)
C(5)	0.1276(1)	0.2120(2)	0.0739(1)	0.0200(3)
C(6)	0.1981(1)	0.2601(2)	0.0981(1)	0.0234(4)
C(7)	0.2125(1)	0.4120(3)	0.1389(1)	0.0235(4)
C(8)	0.1576(1)	0.5182(2)	0.1607(1)	0.0198(3)
C(9)	0.0818(1)	0.4677(2)	0.1427(1)	0.0164(3)
C(10)	−0.0055(1)	0.7038(2)	0.1973(1)	0.0236(4)
C(11)	−0.1270(1)	0.4751(3)	0.0994(1)	0.0260(4)
C(12)	0.1109(1)	0.0561(3)	0.0268(1)	0.0280(4)
C(13)	0.1781(1)	0.6857(3)	0.1913(2)	0.0298(4)

Table 8
Fractional atomic coordinates and equivalent isotropic thermal parameters with estimated standard deviations for the compound $C_{25}H_{26}Cl_2Zr{-}CH_2Cl_2$

Atom	x	y	z	U_{eq} (Å^2)
Zr(1)	0.12069(2)	0.23207(2)	0.26176(2)	0.01023(7)
Cl(1)	0.04128(6)	0.00091(5)	0.24286(5)	0.0200(1)
Cl(2)	0.34782(5)	0.23010(6)	0.34546(5)	0.0206(1)
C(1)	−0.0057(2)	0.3992(2)	0.3157(2)	0.0131(3)
C(2)	−0.0835(2)	0.2851(2)	0.3433(2)	0.0147(4)
C(3)	−0.2101(2)	0.2074(3)	0.2912(2)	0.0238(5)
C(4)	−0.2575(3)	0.1031(3)	0.3398(3)	0.0308(6)
C(5)	−0.1849(3)	0.0702(3)	0.4413(3)	0.0303(6)
C(6)	−0.0643(3)	0.1413(2)	0.4932(2)	0.0243(5)
C(7)	−0.0117(2)	0.2485(2)	0.4447(2)	0.0161(4)
C(8)	0.1105(2)	0.3388(2)	0.4828(2)	0.0160(4)
C(9)	0.2158(3)	0.3447(3)	0.5774(2)	0.0240(5)
C(10)	0.3238(3)	0.4418(3)	0.5948(2)	0.0312(6)
C(11)	0.3285(3)	0.5358(3)	0.5206(3)	0.0301(6)
C(12)	0.2283(2)	0.5325(2)	0.4281(2)	0.0229(4)
C(13)	0.1131(2)	0.4335(2)	0.4061(2)	0.0154(4)
C(14)	−0.0290(2)	0.4513(2)	0.1983(2)	0.0155(4)
C(15)	0.0432(2)	0.3649(2)	0.1223(2)	0.0133(3)
C(16)	−0.0075(2)	0.2324(2)	0.0678(2)	0.0154(4)
C(17)	0.0987(2)	0.1735(2)	0.0357(2)	0.0142(4)
C(18)	0.2163(2)	0.2659(2)	0.0695(2)	0.0133(3)
C(19)	0.1830(2)	0.3835(2)	0.1272(2)	0.0138(3)
C(20)	0.3450(2)	0.2497(2)	0.0274(2)	0.0179(4)
C(21)	0.3237(3)	0.2599(3)	−0.1060(2)	0.0284(5)
C(22)	0.3787(3)	0.1159(3)	0.0384(3)	0.0291(5)
C(23)	0.4593(3)	0.3562(3)	0.0959(3)	0.0305(6)
C(24)	0.0274(3)	0.5958(2)	0.2121(2)	0.0250(5)
C(25)	−0.1749(2)	0.4305(3)	0.1401(2)	0.0235(5)
Cl(3)	0.46858(8)	−0.17138(9)	0.39328(8)	0.0424(2)
Cl(4)	0.32440(8)	−0.20550(9)	0.15008(7)	0.0414(2)
C(26)	0.3466(3)	−0.1208(3)	0.2991(3)	0.0367(6)

3.21. X-ray structure of 2 [41]

Crystal data: $C_{26}H_{30}Cl_2SiZr$; crystal size, $0.4 \times 0.4 \times 0.3$ mm; monoclinic; space group, $C2/c$; temperature, 153 K; $a = 1173.3(2)$, $b = 1419.1(4)$ and $c = 1374.7(3)$ pm; $\beta = 92.44(2)°$; $V = 2286.8(9) \times 10^6$ pm^3; $Z = 4$; $d_{calc} = 1.547$ g cm^{-3}; linear absorption coefficient $\mu = 0.779$ mm^{-1} (Mo Kα); 3343 independent reflections; $2\theta_{max} = 60.0°$; number of parameters, 157; final R value, 0.040 (all reflections); program, SHELXL-93.

3.22. X-ray structure of 4 [41]

Crystal data: $C_{26}H_{28}Cl_2Zr$; crystal size, $0.5 \times 0.4 \times 0.3$ mm; monoclinic; space group, $C2/c$; temperature, 153 K; $a = 1794.9(3)$, $b = 832.6(2)$ and $c = 1461.1(3)$ pm, $\beta = 91.73(2)°$; $V = 2182.5(8) \times 10^6$ pm^3; $Z = 4$; $d_{calc} = 1.530$ g cm^{-3}; linear absorption coefficient $\mu = 0.759$ mm^{-1} (Mo Kα); 3204 independent reflections; $2\theta_{max} = 60.0°$; number of parameters, 150; final R value, 0.038 (all reflections); program, SHELXL-93.

3.23. X-ray structure of 6 [41]

Crystal data: $C_{25}H_{26}Cl_2Zr{-}CH_2Cl_2$; crystal size, $0.5 \times 0.4 \times 0.4$ mm; triclinic; space group, $P\bar{1}$; temperature, 153 K; $a = 1039.9(3)$, $b = 1058.3(3)$ and $c = 1148.9(3)$ pm; $\alpha = 99.29(2)$, $\beta = 98.50(2)$ and $\gamma = 99.03(2)°$; $V = 1212.7(6) \times 10^6$ pm^3; $Z = 2$; $d_{calc} = 1.571$ g cm^{-3}; linear absorption coefficient $\mu = 0.907$ mm^{-1} (Mo Kα); 7124 independent reflections; $2\theta_{max} = 60.0°$; number of parameters, 314; final R value, 0.045 (all reflections); program, SHELXL-93.

References and notes

[1] W. Kaminsky, K. Külper, H.H. Brintzinger and F.R.P.W. Wild, *Angew. Chem., 97* (1985) 507.
[2] F.R.W.P. Wild, M. Wasiucionek, G. Huttner and H.H. Brintzinger, *J. Organomet. Chem., 288* (1985) 63.
[3] W.A. Herrmann, J. Rohrmann, E. Herdtweck, W. Spaleck and A. Winter, *Angew. Chem., 110* (1989) 1536.
[4] W. Spaleck, M. Antberg, V. Dolle, R. Klein, J. Rohrmann and A. Winter, *New J. Chem., 14* (1990) 499.
[5] W. Spaleck, M. Antberg, J. Rohrmann, A. Winter, B. Bachmann, P. Kiprof, J. Behm and W.A. Herrmann, *Angew. Chem., 104* (1992) 1373.
[6] D.R. Burfield, P.S.T. Loi, Y. Doi and J. Mejzik, *J. Appl. Polym. Sci., 41* (1990) 1095.
[7] K. Soga, T. Shiono, S. Takemura and W. Kaminsky, *Makromol. Chem., Rapid Commun., 8* (1987) 305.
[8] B. Rieger, X. Mu, D.T. Mullin, M.D. Rausch and J.C.W. Chien, *Macromolecules, 23* (1990) 3559.
[9] W. Kaminsky and G.U. Schupfner *J. Mol. Catal.*, submitted for publication.
[10] W. Spaleck, F.K. Külper, A. Winter, J. Rohrmann, B. Bachmann, M. Antberg, V. Dolle and E.F. Paulus, *Organometallics, 13* (1994) 954.
[11] U. Stehling, J. Diebold, R. Kirsten, W. Röll, H.-H. Brintzinger, S. Jüngling, R. Mühlhaupt and F. Langhauser, *Organometallics, 13* (1994) 964.
[12] J.A. Ewen, R.L. Jones and A. Razavi, *J. Am. Chem. Soc., 110* (1988) 6255.
[13] J.A. Ewen, M.J. Elder, R.L. Jones, S. Curtis and H.N. Cheng, in T. Keii, K. Soga (eds.), *Catalytic Olefin Polymerization*, Kodansha, Tokyo, 1991, p. 439.
[14] J.A. Ewen, M.J. Elder, R.L. Jones, L. Haspeslagh, J.L. Atwood, S.G. Bott, K. Robinson, *Makromol. Chem., Makromol. Symp., 48–49* (1991) 253.
[15] J.A. Ewen and M.J. Elder (Fina Technology), *Eur. Par. EP-A1-0537130*, 1993; *Chem. Abstr., 119* (1993) 250 726z.
[16] R.T. Hart and R.F. Tebbe, *J. Am. Chem. Soc., 72* (1950) 3286.
[17] Pl. A. Plattner, A. Fürst and H. Schmid, *Helv., 28* (1945) 1647.
[18] J.H. Teles and G. Maier, *Chem. Ber., 122* (1989) 745.
[19] W. Herz, *J. Am. Chem. Soc., 75* (1952) 73.
[20] D. O'Hare, J.C. Green, T. Marder, S. Collins, G. Stringer, A.K. Kakkar, N. Kaltsoyannis, A. Kuhn, R. Lewis, C. Mehnert, P. Scott, M. Kurmoo and S. Pugh, *Organometallics, 11* (1992) 48.
[21] H.W. Pinnick, S.P. Brown, E.A. McLean and L.W. Zoller, *J. Org. Chem., 46* (1981) 3758.
[22] J.M. Conia and M.L. Leriverend, *Bull. Soc. Chem. Fr., 8–9* (1970) 2981.
[23] H.R. Snyder and C.T. Elston, *J. Am. Chem. Soc., 77* (1954) 364.
[24] F.-H. Marquardt, *Helv., 48* (1965) 1476.
[25] A. Razavi and J. Ferrara, *J. Organomet. Chem., 435* (1992) 299.
[26] A. Winter, M. Antberg, V. Dolle, J. Rohrmann and W. Spaleck (Hoechst AG) *Eur. Par. EP-A1-0537686*, 1994; *Chem. Abstr., 120* (1994) 165 214.
[27] L.M. Lee, W.J. Gauthier, J.M. Ball, B. Iyengar and S. Collins, *Organometallics, 11* (1992) 2115.
[28] R. Engehausen, *Dissertation*, Universität Hamburg, 1994.
[29] W. Kaminsky, R. Engehausen, K. Zoumis, W. Spaleck and J. Rohrmann, *Makromol. Chem., 193* (1993) 1643.
[30] J.C.W. Chien, G.H. Llinas, M.D. Rausch, G.-Y. Lin and H.H. Winter, *J. Am. Chem. Soc., 113* (1991) 8569.
[31] E.J. Corey and J.C. Bailar, *J. Am. Chem. Soc., 82* (1959) 2620.
[32] K.F. Purcell and J.C. Kotz, *Inorganic Chemistry*, Holt–Saunders, 1985, p. 636.
[33] geNMR V 3.51, IvorySoft, Amerbos 330, 1025 ZV Amsterdam, Netherlands.
[34] Discover® 2.9 and Insight® II, V 2.3.0., Biosym Technologies, 9685 Scranton Road, San Diego, CA 92121-4778, USA.
[35] Force field parameters were optimized by a fitting procedure to 30 zirconocene complexes [36].
[36] G.U. Schupfner, *Dissertation*, Universität Hamburg, 1995.
[37] P. Burger, K. Hortmann and H.-H. Brintzinger, *Makromol. Chem., Makromol. Symp., 66* (1993) 127.
[38] Th.G. Scholte, N.L.J. Meijerink, H.M. Schoffleers and A.M.G. Brands, *J. Appl. Polym. Sci., 29* (1984) 3763.
[39] R. Riemschneider and R. Nehring, *Monatsh. Chem., 90* (1959) 568.
[40] K.J. Stone and D. Little, *J. Org. Chem., 49* (1984) 1849.
[41] Die jeweils vollständigen Datensätze wurden beim Fachinformationszentrum Karlsruhe, Gesellschaft für wissenschaftlich-technische Information mbH, D-76344 Eggenstein-Leopoldshafen 2, unter den Nummern CSD-401532, CSD-401533, CSD-401534 und CSD-401535 hinterlegt und können von dort unter Angabe der Hinterlegungsnummer, der Autoren und des Zeitschriftenzitats angefordert werden.
[42] G.M. Sheldrick, *SHELXL-93: A Program for the Refinement of Crystal Structures*, University of Göttingen, Göttingen, 1993.